

Geochemistry of a dry steam geothermal zone formed during rapid uplift of Nanga Parbat, northern Pakistan

D. Craw^{a,*}, C.P. Chamberlain^b, P.K. Zeitler^c, P.O. Koons^a

^a *Geology Department, University of Otago, P.O. Box 56, Dunedin, New Zealand*

^b *Department of Earth Sciences, Dartmouth College, Hanover, NH 03755, USA*

^c *Department of Earth and Environmental Sciences, Lehigh University, Bethlehem, PA 18015, USA*

Received 3 September 1996; accepted 19 May 1997

Abstract

Natural dry steam zones (vapour only) are relatively rare; most geothermal systems contain both liquid and vapour and typically follow a boiling point–depth (BPD) relationship. The Nanga Parbat uplift-driven conductive thermal anomaly results in a geothermal system which follows a BPD relationship at shallow levels, but below about 3 km fluid inclusions show that the hydrothermal fluid is dry steam with fluid densities from 0.36 to as low as 0.07 g/cm³. This dry steam zone may persist down to the brittle–ductile transition. The dry steam has salinities up to 5 wt.% dissolved salts, and up to 22 mole% dissolved CO₂. The dry steam originated as meteoric water high on the slopes of Nanga Parbat, with δ¹⁸O as low as –16‰. Oxygen isotopic exchange with the host rock was facilitated by high temperatures (340° to 450°C) and low fluid densities so that the fluid meteoric isotopic signature was completely obliterated. Hence, quartz veins formed by the migrating dry steam have δ¹⁸O between +9 and +15‰, a range which is indistinguishable from quartz in the host rocks. Quartz vein precipitation from dry steam requires 3 to 5 orders of magnitude greater volume of fluid than typical hydrothermal fluids. The dry steam zone at Nanga Parbat has formed due to near-isothermal depressurization of very hot fluid during rapid tectonic uplift at rates > 3–6 mm/year. © 1997 Elsevier Science B.V.

Keywords: geothermal; Himalaya; tectonics; oxygen isotopes; meteoric water; hydrothermal

1. Introduction

Most of the world's active geothermal systems have formed above shallow magma bodies which induce a locally high geothermal gradient. Circulating meteoric water above this body is boiling at most levels so that the temperature–depth profile for the water follows the boiling point–depth (BPD) curve

for the appropriate fluid composition (Haas, 1971; Henley, 1985). The ratio of liquid to vapour in these systems depends on the enthalpy of the system at various levels, which is in turn dependent on the rock temperature at a given depth (White et al., 1971; Henley et al., 1984). Dry steam is high-enthalpy low-density water vapour which has no coexisting liquid and therefore is removed from the BPD relationship. Dry steam is relatively rare in active geothermal systems, and requires distinctly elevated temperatures at shallow levels in low-permeability

* Corresponding author. FAX: +64 (3) 479 7527; E-mail: dave.craw@stonebow.otago.ac.nz.

rocks (White et al., 1971; Armstead, 1978; Elder, 1981).

The Nanga Parbat geothermal system of northern

Pakistan is relatively unusual in that the high geothermal gradient which drives the system arises due to rapid uplift of hot mid-crustal rocks faster

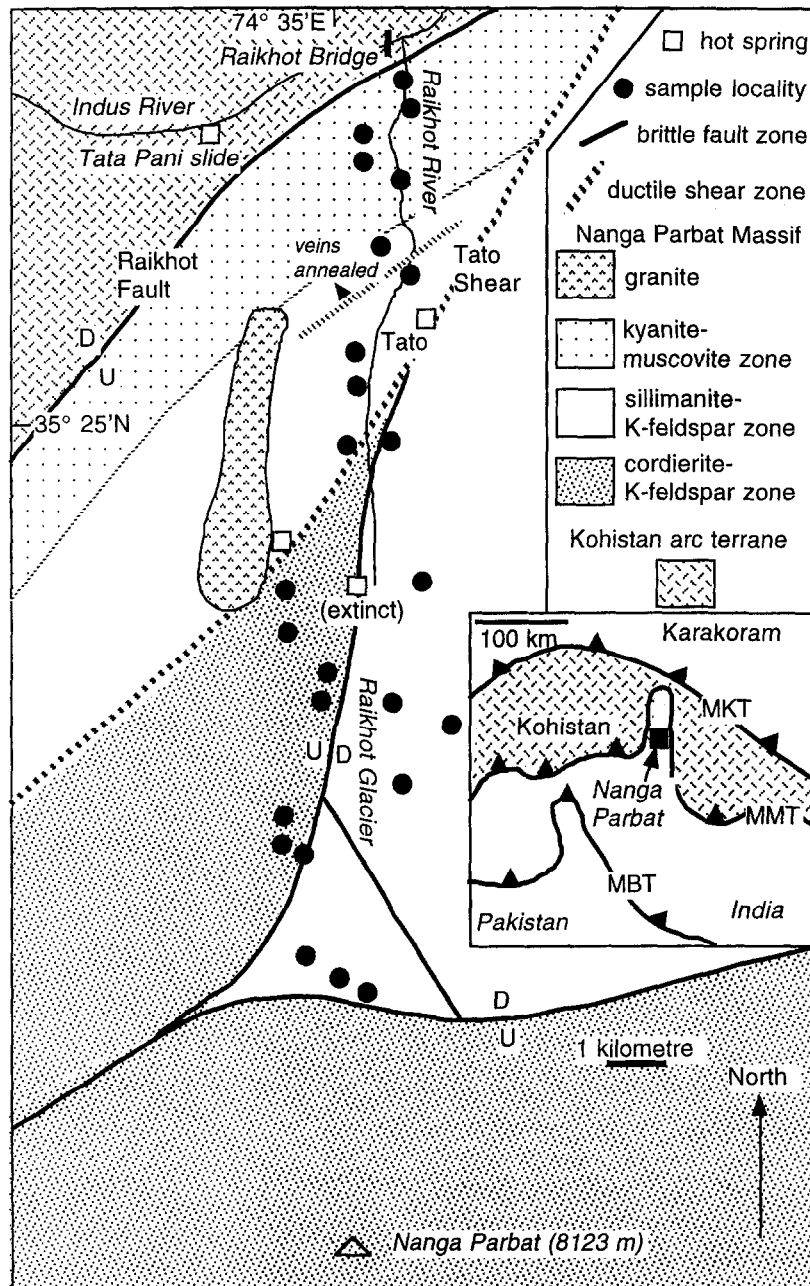


Fig. 1. Geological map showing sample localities in the Raikhot valley traverse into the core of the Nanga Parbat massif, Pakistan. Dashed line north of Tato is approximate boundary of annealed quartz veins in this study (Table 1); dry steam fluid inclusions occur in most veins south of this line. Inset shows the regional geological setting of the Nanga Parbat massif. Regional Himalayan structures: *MKT* = Main Karakoram Thrust; *MMT* = Main Mantle Thrust; *MBT* = Main Boundary Thrust.

than they can cool, and igneous bodies are not necessarily important for heat transfer (Craw et al., 1994). Water in the shallower parts of this geothermal system follows the expected BPD relationship culminating in boiling springs at about 3000 m above sea level. Evidence for the BPD relationship was deduced from study of secondary fluid inclusions in quartz veins (Craw et al., 1994). In addition, some evidence was noted in that study of low-density vapour-rich fluids trapped at depth in the geothermal system. The present study elaborates on this work, and extends it to a study of a wide variety of low-density fluids trapped in primary fluid inclusions in the quartz veins. These low-density fluids are predominantly dry steam, with minor quantities of dissolved salts and/or carbon dioxide. The present study defines the range of fluid compositions and fluid densities, and attempts to place limits on the depths and temperatures at which the dry steam exists. We then examine some of the geochemical consequences of dry steam as a hydrothermal fluid, particularly with respect to stable isotopic interaction with the host rock.

2. General geology

Nanga Parbat is a mountain 8000 m high made up of Precambrian basement of the Indian Plate (Zeitler et al., 1989) in the western Himalayan syntaxis (Fig. 1). The Nanga Parbat massif consists of migmatitic quartzofeldspathic gneisses with minor calcareous gneisses and amphibolites. The massif has been uplifted about 30 km during the Himalayan collision, with about 15 km of uplift occurring within the past 3 million years (Zeitler et al., 1993). Uplift has occurred partly on the Raikhot Fault which is still active (Butler et al., 1989). Late Cenozoic leucogranite sheets, dykes and veinlets from 1 cm to 50 m form a volumetrically minor part of the massif (< 20%). Migmatite bodies, which are locally pegmatitic, formed due to in situ melting at least in part during late Cenozoic uplift and small (up to 1 km) elliptical or irregular-shaped leucogranite bodies intrude the massif (Zeitler et al., 1993).

The present study focusses on a traverse up the Raikhot valley (Fig. 1). This traverse follows and

crosses prominent late Cenozoic structures (Fig. 1) which define the valley, from the edge of the massif to the core. Because of the presence of these structures and the nearby Raikhot Fault (Fig. 1), there has been, and still is, pronounced geothermal activity in the underlying rocks. This geothermal activity is seen at the surface as hot springs or hot spring deposits (Fig. 1), or as alteration zones formed during uplift and erosion (Chamberlain et al., 1995). The geothermal fluids have a meteoric origin and have penetrated into rocks as hot as 500°C (Chamberlain et al., 1995). However, fluid trapped in the basement rocks during the early stages of uplift has a substantial CO₂ content (up to 36 mole%; Winslow et al., 1994).

Samples for this study were obtained from quartz veins which cut the gneiss foliation or young granulites along the Raikhot valley (Fig. 1). Some of these veins have been locally boudinaged and recrystallized (Craw et al., 1994). However, most veins contain subhedral to euhedral quartz, some of which protrudes into open spaces. Quartz is commonly accompanied by biotite and tourmaline. The range of mineralogy and textures of veins is described in detail by Craw et al. (1994), and although the sample set for the present study is larger than that studied by Craw et al. (1994), the same range of vein types was analysed in this study. Not all samples were suitable for fluid inclusion study, and clear quartz was selected as inclusions tend to be larger. Oxygen isotope analyses were conducted on all types of quartz to obtain data over the whole traverse.

3. Primary fluid inclusions

Fluid inclusions were studied petrographically on a standard light microscope using thin and thick sections. Microthermometric data were obtained on a modified USGS gas flow heating/freezing stage at the University of Otago, using doubly polished wafers cut from vein material. Prismatic quartz crystals were cut perpendicular to the prism axis. Heating and cooling conditions were those described by Craw (1988). Some primary inclusion types are similar to secondary inclusions described by Craw et al. (1994). However, most primary inclusion types observed in

this study have not been discussed in detail previously, and these are described in the following section.

Fluid inclusions were examined in samples in which primary inclusions could be clearly recognized (Table 1). However, most of the inclusions in these samples are secondary and occur in oriented trains crossing quartz grains and locally quartz grain

boundaries. These secondary inclusions, which fill healed microfractures (Roedder, 1984), were described in detail by Craw et al. (1994). Confirmation of primary inclusions, which represent the vein-forming fluid rather than later fluid events, is based on textural observations and can be equivocal. Primary inclusions in prismatic quartz crystals are commonly hexagonal, outlining negative crystal shapes, and

Table 1
Quartz vein samples from Raikhot valley

| Sample | Altitude (m) | Host | $\delta^{18}\text{O}(\text{‰})$ | 1° fluid inclusions ^a | | | | |
|-------------|--------------|----------------|---------------------------------|----------------------------------|---------|-------------|----------------------|------------|
| | | | | Texture | T_h | T_m (ice) | $T_{h(\text{CO}_2)}$ | Form T^b |
| PK112b-90 | 2000 | gneiss | 12.5 | | | | | |
| PK1 | 2290 | gneiss | | A | | | | > 450 |
| PK99b-90 | 2300 | gneiss | 11.8 | | | | | |
| PK2 | 2300 | gneiss | | A | | | | > 450 |
| PK3 | 2450 | gneiss | | A | | | | > 450 |
| PK82c-90 | 2500 | gneiss | 11.0 | | | | | |
| PK5 | 2520 | gneiss | 11.1 | A | | | | |
| PK63b-90 | 2600 | gneiss | 11.5 | | | | | |
| PK6 | 2740 | leucogranite | | A | | | | > 450 |
| PK8 | 2850 | gneiss | 13.7 | DS (CO ₂) | 360–380 | | – 11 to – 5 | 360–450 |
| PK404c-92 | 3200 | sheared gneiss | 14.3 | | | | | |
| PK63f-90 | 3300 | leucogranite | 15.6 | | | | | |
| PK9 | 3300 | gneiss | 11.1 | DS (brine) | 390–410 | – 2.0 ± 0.3 | | 390–450 |
| PK10 (a) | 3300 | gneiss | | DS (brine) | 340–350 | – 2.5 ± 0.2 | | 340–450 |
| PK10 (b) | | | | DS (CO ₂) | 390–410 | | + 20 to + 22 | 390–450 |
| PK10 (c) | | | | DS (brine) | 380–395 | – 2.4 ± 0.8 | | 380–450 |
| PK11 | 3350 | gneiss | | WS | 365–380 | – 1.7 ± 0.2 | | 372 ± 7 |
| PK13f-92 | 3400 | leucogranite | 11.1 | | | | | |
| PK132a,b-92 | 3400 | leucogranite | 11.8 | | | | | |
| PK195b-92 | 3500 | gneiss | 13.0 | | | | | |
| PK107b-92 | 3800 | gneiss | 10.9 | | | | | |
| PK121d-92 | 3800 | gneiss | 11.2 | | | | | |
| PK36c-90 | 3800 | leucogranite | 11.4 | | | | | |
| PK12 (a) | 3810 | leucogranite | 13.9 | DS (brine) | 380–405 | – 3.5 ± 1.0 | | 380–450 |
| PK12 (b) | | | | DS (CO ₂) | 390–400 | | + 18 to + 25 | 390–450 |
| PK12 (c) | | | | DS (brine) | 410–415 | – 2.1 ± 0.2 | | 410–450 |
| PK13 | 3810 | leucogranite | | DS (brine) | 390–405 | – 2.1 ± 0.3 | | 390–450 |
| PK14 | 3930 | gneiss | | WS | 378–390 | – 1.8 ± 0.3 | | 384 ± 6 |
| PK15 | 4400 | gneiss | | DS (CO ₂) | 380–400 | | + 21 to + 26 | 380–450 |
| PK16 | 4410 | gneiss | | DS (CO ₂) | 385–395 | | + 10 to + 12 | 385–450 |
| PK17 | 4410 | gneiss | 12.4; 11.4 | DS (brine) | 370–390 | – 2.8 ± 1.2 | | 370–450 |
| PK18 | 4558 | leucogranite | 9.6 | DS (brine) | 390–410 | – 3.1 ± 0.3 | | 390–450 |
| PK19 | 4558 | gneiss | | | | | | |
| PK20 | 4558 | gneiss | | | | | | |
| PK21 | 4400 | gneiss | | DS (brine) | 390–405 | – 2.4 ± 0.2 | | 390–450 |
| PK23 | 3840 | leucogranite | 10.4 | DS (brine) | 400–410 | – 2.7 ± 0.4 | | 400–450 |
| PK404 | 3110 | gneiss | | | | | | |

^a Primary inclusions were not recognized in all samples. Abbreviations: A = annealed; DS = dry steam; WS = wet steam; T_h = homogenization temperature for inclusions; T_m (ice) = ice melting temperature; $T_{h(\text{CO}_2)}$ = carbon dioxide homogenization temperature.

^b 450°C is assumed to be brittle–ductile transition (see text).

distributed randomly through clear quartz. Randomly distributed spherical or ellipsoidal inclusions in anhedral clear quartz are also assumed to be primary. No primary inclusions can be found in deformed veins which occur mainly in the northern part of the Raikhot valley (Fig. 1), since deformation-induced recrystallization has removed all trace of primary fluid.

A variety of primary inclusion compositions can be recognized amongst the studied samples, but the composition is generally uniform within any one wafer. Clusters of 30 or more primary inclusions of uniform composition located within less than 1 mm² on the wafers were examined microthermometrically to determine the nature of the mineralizing fluid. Two samples examined have different compositions of primary inclusions in different wafers cut from the same specimen (Table 1). All inclusions are dominated by water, with variable but small amounts of dissolved salts and CO₂. This study concentrates on dry steam inclusions which are uniform in composition, and show no evidence of boiling during entrapment. However, two samples (PK 11, PK 14; Table 1) contain primary inclusions with variable compositions indicative of entrapment of immiscible fluids during boiling (wet steam) (cf. Craw et al., 1994). Homogenization temperatures determined from expansion of vapour bubbles are not as precise as those obtained from shrinkage of vapour bubbles because of optical effects on inclusion margins. Hence, dry steam homogenization temperatures (Table 1) are quoted to the nearest 5°C. Clusters of up to 40 primary inclusions in the same wafer generally homogenize within < 20°C of each other.

4. Dry steam inclusion compositions

4.1. Brine inclusions

Brine inclusions contain up to 70 vol.% vapour, and homogenize to vapour between 340° and 415°C (Table 1). Freezing point depression is between 1.5° and 4.5°C over all samples examined, with variation within many samples of only 0.2–0.3°C. Some of this freezing point depression (up to 1.5°C; Heden-

quist and Henley, 1985) is undoubtedly due to dissolved CO₂ but up to 3°C of depression implies about 5 wt.% NaCl equivalent. This upper limit of salinity is confirmed with clathrate melting temperatures near 7°C in several samples, implying 5 wt.% NaCl equivalent salinity and saturation with CO₂ (Collins, 1979).

Densities of brines were estimated using the observed microthermometric data and program MacFlinCor (Brown and Hagemann, 1995). Densities range from about 0.07 to 0.3 g/cm³.

4.2. CO₂-bearing inclusions

CO₂-bearing inclusions consist of three phases at room temperature or after cooling to as low as –11°C, and CO₂ homogenization temperatures ($T_{h(\text{CO}_2)}$) range from –11° to +26°C. The inclusions are dominated by CO₂ vapour (about 70–80 vol.%), with a small annulus of CO₂ liquid separating vapour from an outer film of water. CO₂ melting temperatures are between –56.6 and –57°C, implying negligible quantities of other dissolved gases such as CH₄ or N₂. Clathrate melting temperatures of +7 to +9 imply dissolved salt contents of 1.5 to 5 wt.% NaCl equivalent (Collins, 1979). The inclusions homogenize to vapour at 360° to 410°C.

Fluid compositions and densities were calculated from microthermometric data using program MacFlinCor (Brown and Hagemann, 1995) and the equations of state of Bowers and Helgeson (1983). Three compositions representative of the full range of observed data are depicted in Fig. 2A, showing CO₂ content ranging up to 22 mole%. These fluids are from sample PK8 ($T_{h(\text{CO}_2)} = -11^\circ\text{C}$), sample PK10 ($T_{h(\text{CO}_2)} = +20^\circ\text{C}$) and sample PK16 ($T_{h(\text{CO}_2)} = +10^\circ\text{C}$), whose calculated bulk densities are between 0.25 and 0.36 g/cm³. Approximate positions of the solvi for the estimated compositions (after Takenouchi and Kennedy, 1964; Bowers and Helgeson, 1983) are indicated, with isochores emanating from the solvi at the appropriate homogenization temperatures (Fig. 2A).

The petrographic distinctions between brine inclusions and three-phase CO₂-bearing inclusions (Sections 4.1 and 4.2) presumably result from the limited solubility of CO₂ in water at room temperature, and

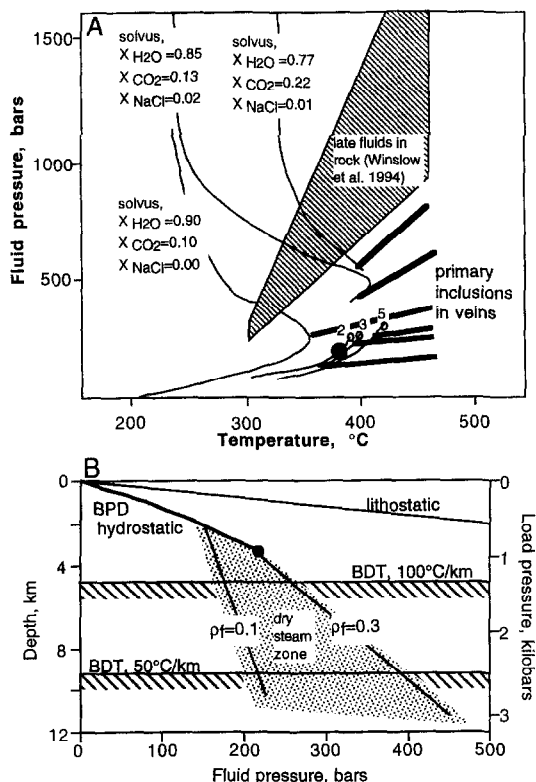


Fig. 2. Phase diagrams for dry steam fluids in primary fluid inclusions, Raikhot valley. (A). Temperature vs. fluid pressure diagram for NaCl brine, and water–NaCl–CO₂ fluids representative of observed compositions (after data and sources in text). Isochores (heavy lines) were calculated for typical dry steam fluids (see text; Table 1) using MacFlinCor (Brown and Hagemann, 1995). Critical points for water (black circle) and brines with 2, 3 and 5 wt.% NaCl (open circles) are indicated at the ends of respective liquid–vapour lines. (B) Fluid pressure vs. depth diagram, showing the lithostatic and hydrostatic BPD curves for pure water, and lines of constant density for the dry steam zone below the hydrostatic BPD curve. Lithostatic brittle–ductile transition (BDT; lines with hatching) depths for average geothermal gradients of 50° and 100°C/km are shown for comparison, assuming the brittle–ductile transition is at 450°C, and these provide theoretical depth limits to the dry steam zone.

a complete range in compositions between limits defined in Sections 4.1 and 4.2 can be observed.

5. Interpretation of temperature and depth of vein formation

Veins which are ductilely deformed and boudinaged have formed under temperature–pressure con-

ditions near to, or greater than, those of the brittle–ductile transition, while those which fill brittle fractures have formed under shallower, probably cooler, conditions. The temperature of this transition is poorly known, and is dependent on strain rate and fluid pressure, but is commonly quoted as about 300–400°C for quartz (Sibson et al., 1979; Knipe, 1989). Primary fluid inclusions in veins filling brittle fractures in this study formed at temperatures greater than 340–415°C (Table 1), and secondary inclusions formed in a similar temperature range (Craw et al., 1994). These temperatures, if indicative of rock temperatures, suggest that the brittle–ductile transition at Nanga Parbat is at least 400°C and possibly higher. The common occurrence of fluid inclusion homogenization temperatures near 400–410°C but not higher than 415°C (Table 1) may indicate that brittle fractures do not form at temperatures higher than this, and the brittle–ductile transition may begin at about this temperature range. A higher temperature limit on brittle fracturing is unconstrained as yet, but we suggest an arbitrary value of 450°C for the purposes of the following discussions. Veins which have been ductilely deformed and annealed presumably formed at temperatures near this arbitrary upper limit: ca. 450°C (Table 1).

Dry steam inclusions with uniform compositions within samples formed at some temperature above their homogenization temperatures along an isochore in *P*–*T* space. Slopes of isochores for representative compositions of CO₂-bearing inclusions (above) have been determined using the method of Bowers and Helgeson (1983) and MacFlinCor (Brown and Hagemann, 1995). Liquid–vapour curves and critical points for representative dry steam brines have been plotted (Fig. 2A) from MacFlinCor, and isochore slopes extrapolated from pure water data (Fisher, 1976). The resultant isochores (Fig. 2A) for primary inclusion fluids define ranges of fluid pressure and temperatures of vein formation. These isochores terminate at 450°C which is taken as the upper limit to unannealed vein formation temperature (above).

Many secondary inclusions formed on the BPD curve (Craw et al., 1994), and some primary fluid inclusions formed on the BPD curve as well (Table 1), so at least some vein mineralization occurred on the BPD curve. Likewise, many primary inclusions and some secondary inclusions include dry steam

(above). Hence, there is a general trend for vein formation initially from dry steam followed by formation at the BPD, with some overlap. The change from dry steam to BPD conditions is due to changes in temperature or fluid pressure (Fig. 2A) which may be local hydrothermal phenomena or responses to tectonic uplift. We cannot resolve the magnitudes or causes of these changes. However, we suggest that vein formation occurred under temperature and fluid pressure conditions near to the BPD curve so that only minor changes in these conditions were required to cause the observed differences in fluid inclusions. If this suggestion is correct, the mineralization temperatures of veins precipitated from dry steam were close to the fluid inclusion homogenization temperatures (Table 1).

Determination of depth of vein formation from fluid pressure estimates (Fig. 2B) requires knowledge of whether the fluid pressure was lithostatic or hydrostatic. Craw et al. (1994) assumed that low-pressure (shallow-level) fluids were hydrostatically pressured, as are most geothermal fields with a BPD relationship (Henley et al., 1984). Dry steam can theoretically exist at a wide range of depths below the BPD zone under hydrostatic conditions, from about 3 to 10 km or even deeper (Fig. 2B, stippled area). The greatest theoretical depth is the base of hydrostatic fluid pressure in the crust, which is assumed to be the brittle–ductile transition, the depth of which depends on the average thermal gradient (Fig. 2B). Nanga Parbat has a strongly elevated thermal gradient (Craw et al., 1994) which has been estimated to be as high as 57°C/km (Winslow et al., 1994), so dry steam can theoretically extend down to about 8 km, assuming that 450°C is the highest temperature at which these veins formed (Fig. 2B). Conversely, if the veins formed from dry steam near to the BPD curve, as was suggested in the previous paragraph, a mineralization depth of 3–4 km is indicated. This latter estimate is plausible but unconstrained.

It is notable that the range of fluid pressures for different samples (Fig. 2A) does not necessarily imply different depths of origin (Fig. 2B). Rather, the differing fluid pressures may have arisen due to differing compositions (and densities) of fluids, trapped at approximately the same depth. Hence, interpretation of the set of isochores in Fig. 2A as

defining an uplift pressure–temperature–time path would be erroneous.

6. Interpretation of composition, density, volume and origin of the dry steam

Dry steam has been observed in primary inclusions in fifteen samples, and as secondary inclusions in another six (Craw et al., 1994). These samples are distributed over a large part of the Raikhot traverse to the south of the zone of annealed veins (Fig. 1). From these observations we conclude that dry steam has been an important mineralizing fluid in the deeper parts of the Raikhot portion of the Nanga Parbat geothermal system. The following paragraphs speculate on the source of that fluid.

Typical upper amphibolite to granulite facies rocks have metamorphic fluids with high CO₂ contents (e.g. Touret, 1981; Fig. 3). Fluids trapped in Nanga Parbat metamorphic basement rocks (not veins) under relatively high fluid pressures (up to 1400 bars) are water–CO₂–salt solutions with up to 36 mole% CO₂ (Winslow et al., 1994; Fig. 3), and may have a substantial component of metamorphic fluid. These deeper Nanga Parbat fluids have a higher CO₂ content than most of the dry steam described in the present study. Conversely, fluids in secondary inclusions in vein quartz are typically even more dilute than the primary dry steam fluids, and some late-stage

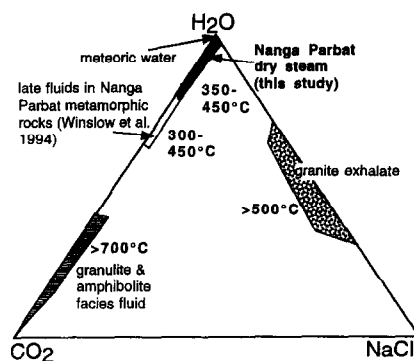


Fig. 3. Observed compositions of dry steam fluids in Nanga Parbat quartz veins (black) in comparison to fluids in Nanga Parbat rocks, and other crustal fluids in high-grade metamorphic complexes (Touret, 1981; Roedder, 1984) or fluid expelled from crystallizing magmas (Roedder, 1984).

secondary boiling or liquid water inclusions formed as shallow as 1–2 km have no detectable dissolved salts or CO₂ (Craw et al., 1994). Hence, there is a general trend in Nanga Parbat fluid compositions with decreasing temperature and depth towards lower solute concentrations. Both primary and secondary inclusions in vein quartz were trapped in the crustal zone inferred to be permeated by circulating meteoric water (Craw et al., 1994; Chamberlain et al., 1995). The observed inclusion compositions are consistent with meteoric origin with increasing (but still minor) amounts of dissolved salts and CO₂ with increasing entrapment depth due to water–rock interaction. All the observed fluids are distinctly different from typical granulite facies metamorphic fluid (Touret, 1981) or fluid expelled from crystallizing magmas (Roedder, 1984; Fig. 3), both of which were presumably present at depth in the Nanga Parbat massif prior to uplift.

Densities of briny dry steam inclusions are low (typically 0.1 to 0.3 g/cm³), and the more carbonic fluids have densities up to 0.36 g/cm³. Secondary inclusions contain vapour-rich fluids which have not boiled, with densities as low as 0.05 g/cm³ (Craw et al., 1994). These vein fluid densities are lower than the 0.37 to 0.85 g/cm³ fluids observed by Winslow et al. (1994) in the host rocks.

Quartz is at least an order of magnitude less soluble in Raikhot valley fluids (1 to 0.1 mmol/kg) than in most hydrothermal solutions (Fournier, 1983). A typical cluster of Raikhot quartz crystals consists of at least 10 moles (600 g) of quartz, and thus would require passage of at least 10⁴ to 10⁵ kg of saturated fluid assuming that all the dissolved silica was deposited in the vein. This equates to at least 10⁵ to 10⁷ l of fluid at the estimated fluid densities, compared to about 700 l of more normal hydrothermal fluid to deposit the same amount of quartz. This combination of low densities and low quartz solubilities requires that the Raikhot hydrothermal system involved passage of very large volumes of low-density fluid.

The Raikhot vein fluid compositions (Fig. 3) and the large volumes of fluid involved in the hydrothermal system at shallow levels strongly suggest that the fluid is meteoric in origin. This is consistent with the occurrence of hot springs in the Raikhot valley area which discharge meteoric water, and meteoric

incursion to magmatic/metamorphic depths beneath Nanga Parbat (Chamberlain et al., 1995). This type of meteoric incursion has been shown to be a normal part of actively rising mountains elsewhere (Nesbitt et al., 1986; Jenkin et al., 1994).

7. Oxygen isotopic analyses of vein quartz

7.1. Isotopic data

Oxygen isotope analyses were conducted on the laser ablation line at Dartmouth College (Conrad and Chamberlain, 1992) using about 1 mg of quartz vein material from each sample, and NBS-28 as a laboratory standard. Only quartz vein material free of weathering limonite was analysed. Results for samples analysed are listed in Table 1 and plotted with geographical position in Fig. 4A.

Quartz δ¹⁸O for most veins lies between +9.6 and +12.8‰ over the whole Raikhot traverse (Fig. 4A). A set of anomalously high values (up to +15.9; Fig. 4A) occurs over the 5 km upstream of Tato village (Fig. 1). There is no isotopic difference between annealed samples found mainly near the Raikhot Fault (Table 1; Fig. 1) and most unannealed samples found farther south. All the anomalously high values are from unannealed quartz in undeformed veins. Veins with visible dry steam primary fluid inclusions span most of the observed range in vein data and are indistinguishable isotopically from other veins (Fig. 4A). The measured vein quartz isotopic data are, apart from one sample, isotopically indistinguishable from the quartz of the basement host rocks (Fig. 4A; Chamberlain et al., 1995), and only four of the anomalous veins are isotopically heavier than the basement whole-rock isotopic range (Fig. 4A).

7.2. Calculated isotopic signatures of fluids

The δ¹⁸O of the vein-forming dry steam can be calculated from the δ¹⁸O of the vein quartz, using the formation temperatures inferred from primary fluid inclusions (above), provided the veins formed in equilibrium with the fluid, and fractionation factors from Matsuhisa et al. (1979). Using a vein formation temperature range of 370–500°C we cal-

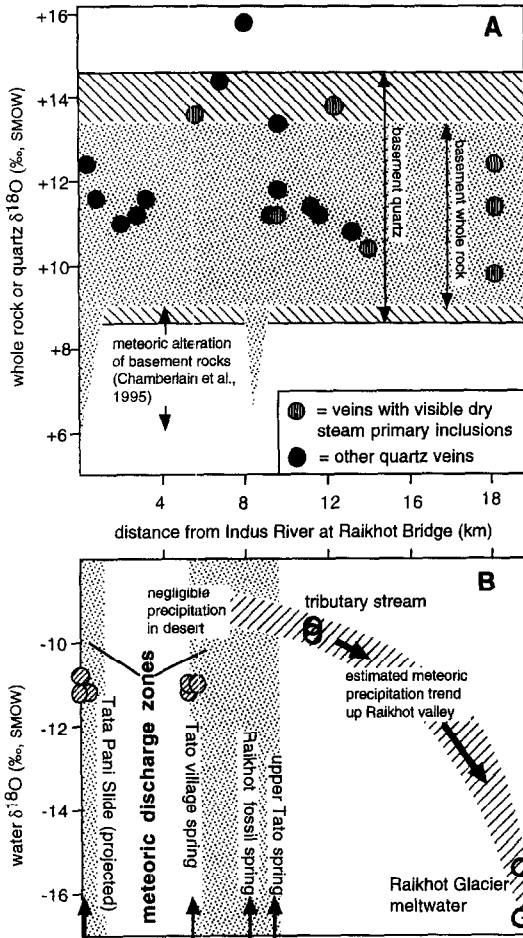


Fig. 4. Oxygen isotope data for the Raikhot valley traverse, plotted against distance from the Indus River at Raikhot Bridge (Fig. 1). (A) Quartz veins (circles) including veins with primary dry steam fluid inclusions (hatched circles) generally fall into the range of data for quartz from basement rocks (hatched) and basement whole-rock data. Meteoritic alteration has resulted in isotopically light zones in the vicinity of the Raikhot Fault and Tato Shear (Fig. 1, and B). (B) Meteoric water oxygen isotope data for streams and springs in the Raikhot valley area. Meteoric discharge zones (approximated by stippled areas) coincide with zones of meteoric alteration of rock in (A).

culate $\delta^{18}\text{O}$ of the water in the fluid to be +4 to +10‰ for most of the veins, and the anomalous veins from near Tato village had water $\delta^{18}\text{O}$ of +8 to +13‰ (Fig. 5). Similarly, the isotopic signature of the fluids in equilibrium with the basement granites and gneisses can be calculated from the $\delta^{18}\text{O}$ of the quartz in these rocks. Isotopic fractionation between quartz and feldspar in granite and gneiss

suggests that these minerals were in isotopic equilibrium between 500° and 700°C in both rock types (Chamberlain et al., 1995). Fluid in equilibrium with granite had water $\delta^{18}\text{O}$ between +7 and +13‰, and water in equilibrium with gneiss had $\delta^{18}\text{O}$ between +10 and +15‰ (Fig. 5).

Meteoric incursion into shear zones in the basement gneisses has resulted in localized decreases in $\delta^{18}\text{O}$ of the rocks down to +6‰, at temperatures as low as 400°C (Chamberlain et al., 1995; Figs. 4 and 5). Water in equilibrium with these altered zones ranges from +10‰ down to +2‰ (Fig. 5). This alteration has resulted from isotopic exchange with circulating meteoric water with $\delta^{18}\text{O}$ between -10 and -16‰ (Chamberlain et al., 1995; Fig. 4B, Fig. 5). Meteoric water $\delta^{18}\text{O}$ is strongly dependent on temperature and therefore altitude of precipitation (Dansgaard, 1964). An estimated profile for meteoric water $\delta^{18}\text{O}$ up the Raikhot valley (Fig. 4B) is based on a measured mid-valley stream with a low altitude source, and on analyses from the Raikhot Glacier which has its source in névés high on the slopes of Nanga Parbat.

7.3. Interpretation of fluid–rock isotopic exchange

There is widespread evidence for voluminous meteoric incursion deep into the Nanga Parbat massif.

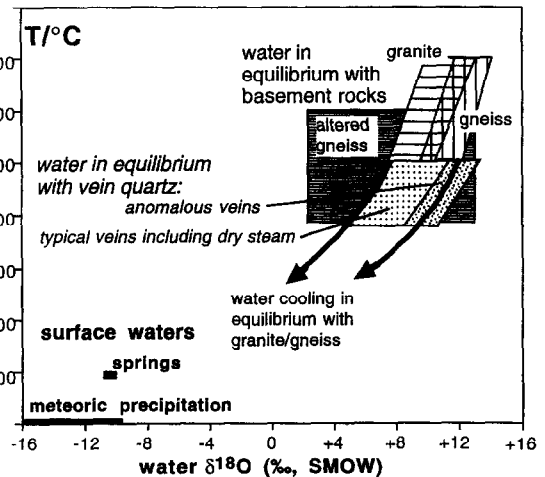


Fig. 5. Calculated isotopic signature of waters in equilibrium with basement rocks and veins, plotted against inferred temperature of equilibration. Surface water data ranges are presented for comparison.

This evidence includes fluid composition (Section 6), isotopic shifts in basement rocks (Chamberlain et al., 1995; Section 7.2), and hot springs discharging meteoric water (Fig. 4B). The Raikhot vein-forming fluids consisted dominantly of this deep-circulating meteoric water (Section 6), but the fluids do not have a meteoric oxygen isotope signature (Section 7.2). Rather, the oxygen isotopic signature of the fluid is essentially identical to fluid which was in isotopic equilibrium with the host rocks and then cooled (Fig. 5). Clearly the originally meteoric fluid has undergone isotopic exchange with the rocks through which it passed. Partial isotopic exchange of meteoric fluid oxygen with rock in this type of environment has been documented previously (Nesbitt et al., 1986; Jenkin et al., 1994), but the Raikhot fluids do not retain any oxygen isotope evidence of their origin.

Equilibrium isotopic exchange between fluid and rock can be calculated in terms of a mass water/rock ratio, R (Ohmoto and Rye, 1974). This time-integrated water/rock ratio represents a minimum amount of fluid, as fluid–rock interaction is also kinetically controlled (Blattner and Lassey, 1989), but is a useful parameter when examining progressive isotopic exchange of fluid in contact with rock. The oxygen isotope ratio for water which has exchanged with rock with a given value of R can be calculated provided initial water and rock isotopic ratios, and the temperature of reaction, are known (Ohmoto and Rye, 1974). A model curve (Fig. 6) depicts Nanga Parbat meteoric water evolving isotopically with decreasing R as it moves through Raikhot valley rocks (assumed to be represented isotopically by quartz) at 400°C. This curve suggests that the water approaches the isotopic composition of the rock only under very low mass fluid/rock ratios ($R < 0.01$).

The above calculations do not take into account the very low density of the Raikhot mineralizing fluids, dominated by dry steam. Because of this low density, the number of water molecules in contact with rock at any one time is lower than for more normal hydrothermal solutions, for a given R value. This can be quantified in the above calculations by correcting the oxygen water/rock atomic ratio with water/rock density ratio, and model curves for water densities of 1, 0.1 and 0.01 g/cm³ are presented (Fig. 6). The latter two densities are most relevant to

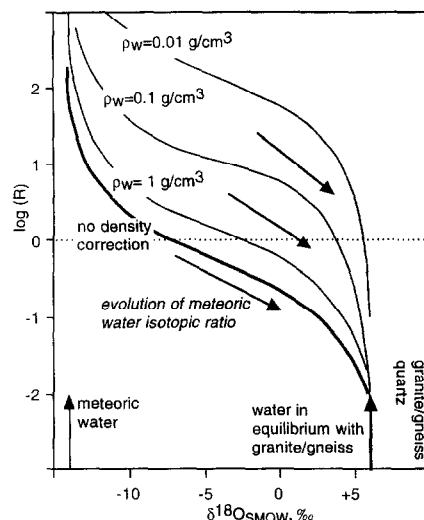


Fig. 6. Modelled variation of oxygen isotope ratio of water with increasing exchange with host rock for fluids of different densities. R = mass water/rock ratio (see text). Dry steam densities are represented by the 0.1 and 0.01 g/cm³ curves (see text).

the Raikhot valley mineralization, and the resultant curves show that water can approach the rock oxygen isotope ratio at $R > 1$, more than 10 times higher water/rock ratio than for more dense 'normal' hydrothermal fluids. Conversely, for a given water/rock mass ratio of, say, $R = 1$, more dense fluids have their oxygen isotope ratios only partially exchanged with that of the rock, while the less dense fluids have fully exchanged and lost their meteoric signature.

We suggest that the model for low-density fluids is representative of the isotopic evolution of Nanga Parbat dry steam (Fig. 6). The anomalously high $\delta^{18}\text{O}$ values observed south of Tato village (Figs. 1 and 4) define the most exchanged meteoric water which was being discharged in a zone where shallower meteoric water emanates as hot springs and rock isotopic analyses indicate substantial penetration of meteoric water into hot ($> 400^\circ\text{C}$) rock (Chamberlain et al., 1995). This part of the valley was, and is, an important meteoric fluid discharge zone. Calculated water $\delta^{18}\text{O}$ values spread down towards $+4\text{‰}$ for data elsewhere in the valley (Fig. 5). This could be due to the effects of inherent host rock $\delta^{18}\text{O}$ range coupled with complete evolution of meteoric water $\delta^{18}\text{O}$ to that of the rock. Alterna-

tively, there may have been only partial water $\delta^{18}\text{O}$ evolution towards rocks with initial high $\delta^{18}\text{O}$.

8. Nanga Parbat uplift and dry steam generation

The presence of a dry steam zone, a rare occurrence, beneath the Nanga Parbat geothermal system implies that the geological processes at Nanga Parbat are unusual compared to most geothermal systems. One outstanding feature of Nanga Parbat geology is the current rapid uplift which is reputed to be one of the fastest tectonic uplift zones on Earth (Zeitler et al., 1993). Bedrock incision rates as high as 12 mm/year have been suggested in the Indus River gorge about 50 km to the north (Burbank et al., 1996). Thermochronological data for the upper Raikhot valley suggest denudation rates of 3–6 mm/year (Zeitler et al., 1993; Winslow et al., 1994), and since the area is now 3–4 km above sea level, rock uplift rates could be even higher.

Given the high uplift rates, the thermal structure beneath Nanga Parbat inevitably evolved towards a substantial conductive thermal anomaly (Koons, 1987; Craw et al., 1994; Winslow et al., 1996). Rocks uplifted through this anomaly must undergo almost isothermal uplift to within a few kilometres of the surface, and then rapid cooling. Fluid carried with these rocks or percolating upwards will be the same temperature as the host rock provided fluid movement is slow, highly likely in low-permeability rocks near the brittle–ductile transition (Ingebritson and Hayba, 1994). Near-isothermal pressure drop of low-density supercritical saline water near the critical point results in increase in enthalpy (Elder, 1981; Ingebritson and Hayba, 1994) and formation of dry steam. Hence, the extremely rapid tectonic uplift causes the shallow thermal anomaly, the near-surface BPD geothermal system, and possibly the isothermal depressurization of slowly migrating meteoric water beneath the geothermal system, all of which contribute to formation of the dry steam zone beneath the Raikhot valley.

9. Conclusions

Rapid rock uplift of Nanga Parbat of more than 3–6 mm/year has resulted in a pronounced thermal

anomaly. Meteoric fluid penetrates several kilometres into this anomalous thermal zone and can be heated to at least 415°C while interacting with the host gneisses and granites. Rising meteoric fluid produces near-surface hydrothermal activity and surface hot springs. This near-surface geothermal system follows the boiling point–depth (BPD) relationship typical of most geothermal systems. However, beneath the BPD zone, a dry steam zone has formed in the core of the Nanga Parbat massif at depths in excess of 3 km and extends possibly as deep as the brittle–ductile transition. In this dry steam zone briny vapour (up to 5 wt% dissolved salts) and CO_2 -bearing saline water vapour pervades the rock and has deposited quartz veins in fractures.

The dry steam has low density, from 0.36 g/cm³ down to 0.07 g/cm³, distinctly lower than fluids which pervade the host rock at greater depths. The dry steam zone has probably arisen due to depressurization of the fluid during near-isothermal uplift in the thermal anomaly. Dry steam interaction with the host rock has resulted in complete oxygen isotope exchange between fluid and rock, so that the meteoric isotopic signature has been obliterated. This isotopically exchanged fluid is not recognizable at the surface as it is diluted by more voluminous unexchanged meteoric water which emanates from hot spring systems.

Acknowledgements

Field work for this study was supported financially by NSF Grant EAR 9105878 and the University of Otago. Discussions with R.J. Norris and D. Winslow have helped to develop and clarify ideas expressed. Expert technical assistance by B. Pooley in production of polished wafers was much appreciated. The manuscript was significantly improved by constructive criticism by D.O. Hayba and an anonymous referee.

References

- Armstead, H.C.H., 1978. *Geothermal Energy*. Spon, London, 357 pp.
- Blattner, P., Lassey, K.R., 1989. Stable isotope exchange fronts,

- Damköhler Numbers and fluid to rock ratios. *Chem. Geol.* 78, 381–392.
- Bowers, T.S., Helgeson, H.C., 1983. Calculation of the thermodynamic consequences of non-ideal mixing in the system $\text{H}_2\text{O}-\text{CO}_2-\text{NaCl}$ on phase relations in geologic systems. *Metamorphic equilibria at high pressures and temperatures. Am. Mineral.* 68, 1059–1075.
- Brown, P.H., Hagemann, S.G., 1995. MacFlinCor and its application to fluids in Archean lode-gold deposits. *Geochim. Cosmochim. Acta* 59, 3943–3952.
- Burbank, D.W., Leland, J., Fielding, E., Anderson, R.S., Brozovic, N., Reid, M.R., Duncan, C., 1996. Bedrock incision, rock uplift and threshold hillslopes in the northwest Himalayas. *Nature* 379, 505–510.
- Butler, R.W.H., Prior, D.J., Knipe, R.J., 1989. Neotectonics in the Nanga Parbat syntaxis, Pakistan, and crustal stacking in the northwest Himalayas. *Earth Planet. Sci. Lett.* 94, 329–343.
- Chamberlain, C.P., Zeitler, P.K., Barnett, D.E., Winslow, D., Poulson, S.R., Leahy, T., Hammer, J.E., 1995. Active hydrothermal systems during the recent uplift of Nanga Parbat. *J. Geophys. Res.* 100, 439–453.
- Collins, P.L.F., 1979. Gas hydrates in CO_2 -bearing fluid inclusions and the use of freezing data for estimation of salinity. *Econ. Geol.* 74, 1435–1444.
- Conrad, M.E., Chamberlain, C.P., 1992. Laser-based, in situ measurements of fine-scale variations in the $\delta^{18}\text{O}$ values of hydrothermal quartz. *Geology* 20, 812–816.
- Craw, D., 1988. Shallow-level metamorphic fluids in a high uplift rate mountain belt, Alpine Schist, New Zealand. *J. Meteorol. Geol.* 6, 1–16.
- Craw, D., Koons, P.O., Winslow, D., Chamberlain, C.P., Zeitler, P., 1994. Boiling fluids in a region of rapid uplift, Nanga Parbat massif, Pakistan. *Earth Planet. Sci. Lett.* 128, 169–182.
- Dansgaard, W., 1964. Stable isotopes in precipitation. *Tellus* 16, 436–468.
- Elder, J., 1981. *Geothermal Systems*. Academic Press, London, 508 pp.
- Fisher, J.R., 1976. The volumetric properties of H_2O : a graphical portrayal. *U.S. Geol. Surv. J. Res.* 4, 189–193.
- Fournier, R.O., 1983. A method of calculating quartz solubilities in aqueous sodium chloride solutions. *Geochim. Cosmochim. Acta* 47, 579–586.
- Haas, J.L., 1971. The effect of salinity on the maximum thermal gradient of a hydrothermal system at hydrostatic pressures. *Econ. Geol.* 66, 940–946.
- Hedenquist, J.W., Henley, R.W., 1985. The importance of CO_2 on freezing point measurements of fluid inclusions: Evidence from active geothermal systems and implications for epithermal ore deposition. *Econ. Geol.* 80, 1379–1406.
- Henley, R.W., 1985. The geothermal framework of epithermal systems. In: Berger, B.R., Bethke, P.M. (Eds.), *Geology and Geochemistry of Epithermal Systems*. *Rev. Econ. Geol.* 2, 1–24.
- Henley, R.W., Truesdell, A.H., Barton, P.B., 1984. Fluid-mineral equilibria in hydrothermal solutions. *Rev. Econ. Geol.* 1, 267 pp.
- Ingebritsen, S.E., Hayba, D.O., 1994. Fluid flow and heat transport near the critical point of H_2O . *Geophys. Res. Lett.* 21, 2199–2202.
- Jenkin, G.R.T., Craw, D., Fallick, A.E., 1994. Stable isotope and fluid inclusion evidence for meteoric fluid penetration into an active mountain belt; Alpine Schist, New Zealand. *J. Metamorph. Geol.* 12, 429–444.
- Knipe, R.J., 1989. Deformation mechanisms—recognition from natural tectonites. *J. Struct. Geol.* 11, 127–146.
- Koons, P.O., 1987. Some thermal and mechanical consequences of rapid uplift; an example from the Southern Alps, New Zealand. *Earth Planet. Sci. Lett.* 86, 307–319.
- Matsuhisa, Y., Goldsmith, J.R., Clayton, R.N., 1979. Oxygen isotopic fractionation in the system quartz–albite–anorthite–water. *Geochim. Cosmochim. Acta* 43, 1131–1140.
- Nesbitt, B.E., Murowchick, J.B., Muehlenbachs, K., 1986. Dual origins of lode gold deposits in the Canadian Cordillera. *Geology* 14, 506–509.
- Ohmoto, H., Rye, R.O., 1974. Hydrogen and oxygen isotopic compositions of fluid inclusions in the Kuroko deposits, Japan. *Econ. Geol.* 69, 947–953.
- Roedder, E., 1984. *Fluid Inclusions*. *Min. Soc. Am. Rev. Mineral.*, Washington, D.C. 12, 644 pp.
- Sibson, R.H., White, S., Atkinson, B.K., 1979. Fault rock distribution and structure within the Alpine Fault zone: a preliminary account. In: Walcott, R.I., Cresswell, M.M. (Eds.), *The Origin of the Southern Alps*. *Bull. R. Soc. N.Z.* 18, 55–66.
- Takenouchi, S., Kennedy, G.C., 1964. The binary system $\text{H}_2\text{O}-\text{CO}_2$ at high temperatures and pressures. *Am. J. Sci.* 262, 1055–1074.
- Touret, J., 1981. Fluid inclusions in high grade metamorphic rocks. In: Hollister, L.S., Crawford, M.L. (Eds.), *Fluid Inclusions: Applications to Petrology*. *Miner. Assoc. Can. Short Course Handb.* 6, 182–208.
- White, D.E., Muffler, L.J.P., Truesdell, A.H., 1971. Vapor-dominated hydrothermal systems compared with hot water systems. *Econ. Geol.* 66, 75–97.
- Winslow, D.M., Zeitler, P.K., Chamberlain, C.P., Hollister, L.S., 1994. Direct evidence for a steep geotherm under conditions of rapid denudation, Western Himalaya, Pakistan. *Geology* 22, 1075–1078.
- Winslow, D.M., Zeitler, P.K., Chamberlain, C.P., Williams, I.S., 1996. Geochronological constraints on syntaxial development in the Nanga Parbat region, Pakistan. *Tectonics* 15, 1292–1308.
- Zeitler, P.K., Sutter, J.F., Williams, I.S., Zartman, R.E., Tarikheli, R.A.K., 1989. Geochronology and temperature history of the Nanga Parbat–Haramosh Massif, Pakistan. In: Malinconico, L.L., Lillie, R.J. (Eds.), *Tectonics of the Western Himalayas*. *Spec. Pap. Geol. Soc. Am.* 232, 1–23.
- Zeitler, P.K., Chamberlain, C.P., Smith, H.A., 1993. Synchronous anatexis, metamorphism, and rapid denudation at Nanga Parbat (Pakistan Himalaya). *Geology* 21, 347–350.